

Classification  
Physics Abstracts  
07.80 — 82.80 — 75.90

## Iron $L_{2,3}$ white line ratio in nm-sized $\gamma$ -iron crystallites embedded in MgO

Hiroki Kurata<sup>(1)</sup> and Nobuo Tanaka<sup>(2)</sup>

<sup>(1)</sup> Institute for Chemical Research, Kyoto University, Uji, Kyoto-fu 611, Japan

<sup>(2)</sup> Department of Applied Physics, School of Engineering, Nagoya University, Chikusa-ku, Nagoya 464-01, Japan

(Received October 15, 1990; accepted March 28, 1991)

**Abstract.** — Electron energy loss spectroscopy has been performed on nanometer-sized  $\alpha$ - and  $\gamma$ -iron crystallites embedded in single-crystal MgO films prepared by vacuum-codeposition of iron and MgO. The Fe  $L_3/L_2$  white line ratio of  $\gamma$ -iron crystallites was found to be slightly larger than the white line ratio of  $\alpha$ -iron. This suggests that nm-sized  $\gamma$ -iron crystallites embedded in single-crystal MgO are in a high-spin state similar to  $\alpha$ -iron, and is consistent with previous magnetization measurements of  $\gamma$ -iron/MgO composite films

### 1. Introduction.

Resonance peaks (white lines) appearing at the threshold of L and M edges in EELS or XAS spectra can be a rich source of information on the electronic structure of materials. Following the first observation of an anomaly in the  $L_3/L_2$  white line intensity ratio in 3d-transition metals and oxides [1], several experimental and theoretical studies of the ratio have been reported [2-9]. For instance, Morrison *et al.* investigated the iron  $L_{2,3}$ -edge in amorphous alloys and found that decreasing the iron magnetic moments by alloying leads to a decrease of the white line ratio [6,7]. This indicates that a careful analysis of the white line intensities should yield information on the magnetic properties of many different materials.

In the present study, electron energy loss spectroscopy was performed on nanometer-sized  $\alpha$ - and  $\gamma$ -iron crystallites embedded in a thin film of MgO, in order to investigate the magnetic state of  $\gamma$ -iron in the composite material.

### 2. Experimental.

The  $\gamma$ -iron crystallites studied here were found in the course of an investigation of Fe/single crystal MgO composite films prepared by simultaneous vacuum co-deposition [10]. Iron and MgO were evaporated in a UHV chamber at  $10^{-6}$  Pa pressure, from a tungsten-boat and an electron heating gun, respectively. The substrate was a (001) cleaved surface of sodium chloride heated to 350°C.

The deposition rates of iron and MgO were 0.1 to 2.0 nm/s and 0.5 to 2.0 nm/s, respectively. The thickness of the composite film was 2 to 5 nm. In order to cover the  $\gamma$ -iron crystallites completely, pure MgO of 10 nm thickness was deposited before and after the co-deposition. Total thickness of the samples was therefore about 22 to 25 nm. The films were separated from the substrate in water, and a structural characterization was performed in a 200 kV high resolution electron microscope (JEM-2010). Full details of the preparation procedure have been described in a previous paper [10].

Electron energy loss spectra were recorded using a Gatan 666-PEELS attached to a transmission electron microscope (JEM-2000FXII) operating in diffraction mode at 200 kV. Data collection and analysis were performed using Gatan EL/P software running on a Macintosh II computer. Spectra were obtained from areas of about  $2 \mu\text{m}$  in diameter with integration times of 20 sec. The collection angle was defined by the entrance aperture of the spectrometer, and was about 3 mrad. The samples were found to be thin enough for multiple scattering to have only a minimal effect on the detailed edge shapes, and deconvolution of the measured spectra was therefore not performed.



Fig. 1. — High-resolution electron micrograph (a) and diffraction pattern (b) of  $\gamma$ -iron crystallites embedded in an MgO single crystal film. Note the deformation of the interface regions between the  $\gamma$ -iron and the MgO (arrows).

### 3. Results and discussion.

Figures 1a and 1b show a high-resolution electron micrograph and a diffraction pattern, both recorded at room temperature, of  $\gamma$ -iron crystallites epitaxially embedded in a [001]-oriented thin MgO single-crystal film. The diffraction pattern confirms the presence of iron with an f.c.c. structure, and indicates that there were no iron oxides present. It shows the lattice constant of the  $\gamma$ -iron crystallites to be  $0.358 \pm 0.015$  nm, in agreement with a value previously observed at 290K [11]. In the micrograph,  $\gamma$ -iron crystallites are identified as particles of about 2 nm in size. The moiré fringes appearing in the crystallites are due to the interference between the (200) diffraction spots of  $\gamma$ -iron and MgO. The (200) lattice fringes at the periphery of the crystallites bend slightly outwards, as indicated by arrows. This is due to the deformation of the (200) lattice planes caused by a lattice misfit of about 15%. From other tilting and cross-sectional observations of the specimen, it was inferred that the shape of the  $\gamma$ -iron crystallites is typically that of a thin plate less than 1 nm in height.

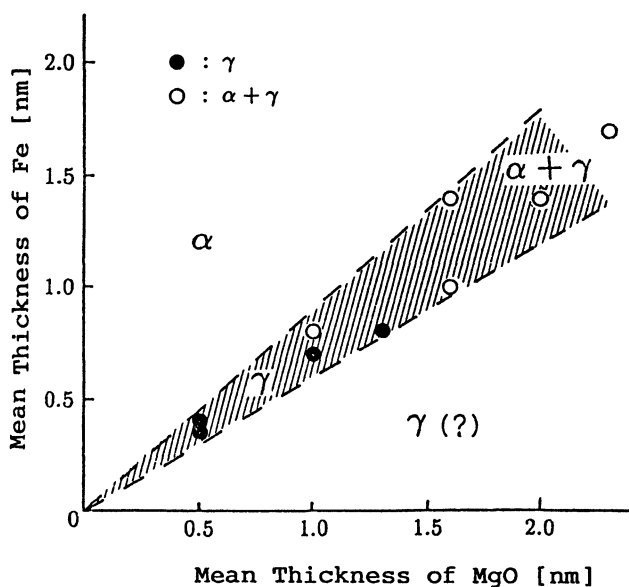


Fig. 2. — Distribution of mean thickness of iron and MgO for which  $\alpha$ - and  $\gamma$ -iron crystallites are identified in diffraction patterns.

Figure 2 shows which iron crystallite phases were found to grow in MgO as a function of the deposition conditions. By changing the deposition ratio of iron against MgO, one can obtain two types of structures in the iron crystallites. The conditions for the growth of  $\gamma$ -iron are (1) the Fe/MgO ratio should be 0.6 to 0.9 (shaded area) and (2) the total thickness of the composite film ( $t_{\text{Fe}} + t_{\text{MgO}}$ ) should be less than a few nm. The type of iron crystallites present was carefully checked, using electron diffraction patterns and moiré fringes in the micrographs for each sample subsequently studied by EELS, and samples with a mixture of  $\alpha$ - and  $\gamma$ -iron crystallites were excluded from the study.

Electron energy loss spectra of iron  $L_{2,3}$  edge measured from  $\alpha$ - and  $\gamma$ -iron crystallites embedded in MgO films are shown in figures 3a and 3b, respectively. In these spectra, the pre-edge

background was subtracted using an  $AE^{-r}$  fit over an energy interval extending 100 eV before the iron  $L_{2,3}$  edge in each spectrum.

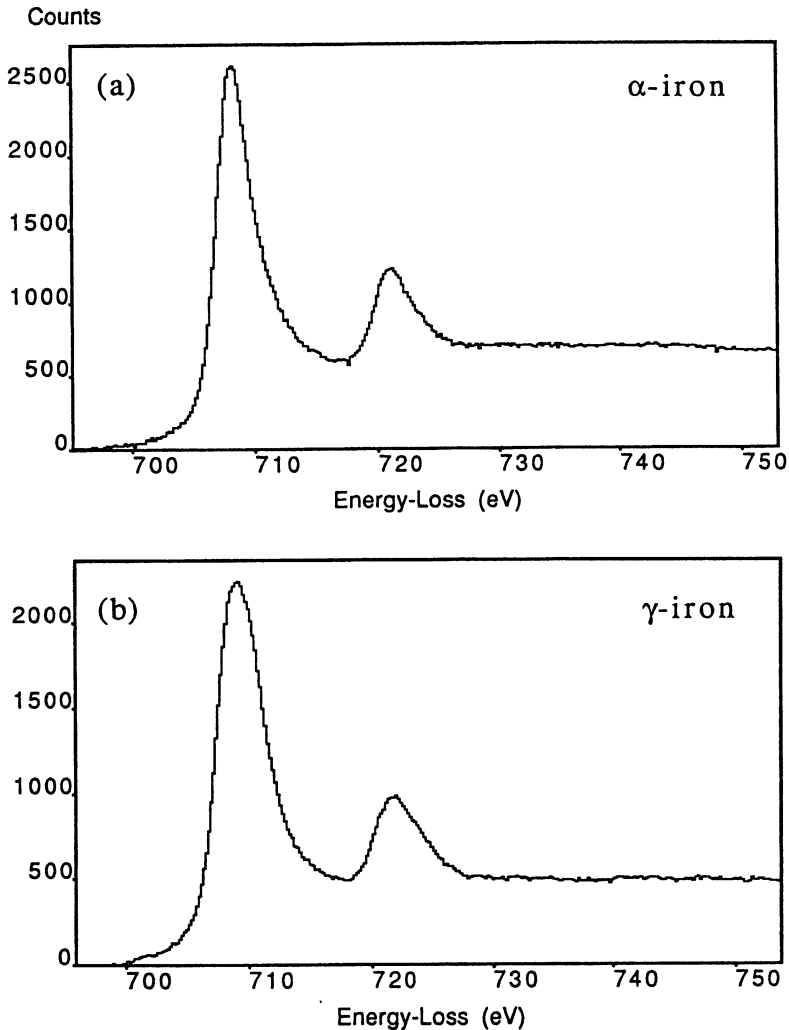


Fig. 3. — Iron  $L_{2,3}$ -edges of  $\alpha$ - and  $\gamma$ -iron crystallites embedded in MgO films after background subtraction.

In order to extract the correct intensities of the white lines, which are due to transitions to a bound state, it is first necessary to remove the contribution to the  $L_{2,3}$ -edge which is due to transitions to the continuum. In previous studies [6-9], several kinds of method of subtracting the continuum have been proposed. In the present paper, we used the following method. The continuum part of the  $L_3$ -edge was first calculated using the hydrogenic model (SIGMAL2) [12]. Next, the  $L_2$  edge was added, with a threshold taken to be 13 eV higher than the  $L_3$  threshold, and an intensity of one half of the  $L_3$  component. The summed  $L_3$  and  $L_2$  components were then fitted to the experimental spectrum over an energy region extending from 740 eV to 790 eV as

shown in figure 4a. The resultant fit was highly satisfactory, confirming that multiple scattering did not have a major influence on the edge shape. Figure 4b shows the white lines obtained by subtracting the continuum part. The intensities of  $L_3$  and  $L_2$  peak were measured by integration over an energy window of 4 eV centered at the respective peaks.

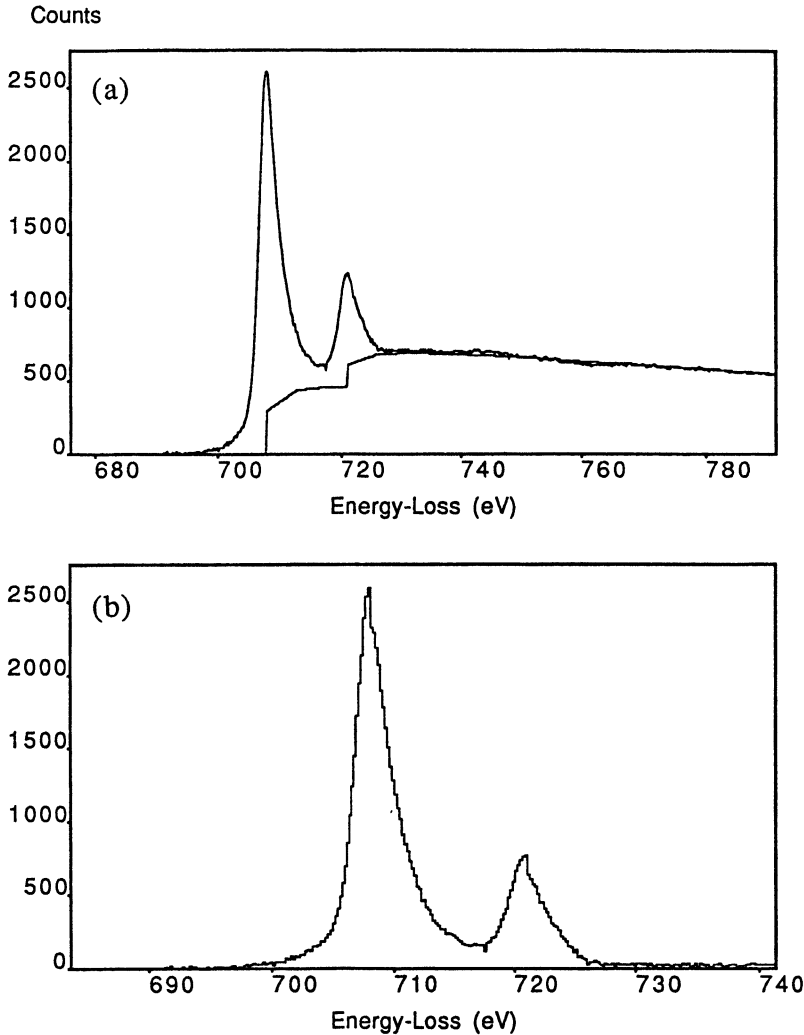


Fig. 4. — Continuum part of  $L_{2,3}$ -edge calculated using the hydrogenic model (SIGMAL2) (a). The  $L_2$  threshold energy is taken to be 13 eV higher than the  $L_3$  threshold, and the  $L_3/L_2$  continuum intensity ratio is taken to be 0.5. The calculated spectrum was fitted to the experimental one over an energy region extending from 740 eV to 790 eV and then subtracted. Figure 4b is the result.

The white line ratio of  $\gamma$ -iron crystallites was thus determined to be 3.5, which is a little larger than in  $\alpha$ -iron, for which the  $L_3/L_2$  ratio was measured to be 3.1. Applying other subtraction methods, in which the edge shape is modeled by a step-function, or a straight line [8], also showed the  $\gamma$ -iron  $L_3/L_2$  ratio to be higher than the  $\alpha$ -iron one.

Because the  $L_{2,3}$  white lines are due to transitions from the  $2p_{1/2}$  and  $2p_{3/2}$  core levels to unoccupied 3d states, the white line ratio should be sensitive to the structure of the d-band [1-9]. Thole and Laan have suggested that a high-spin state leads to a larger white line ratio than a low-spin state of the same material [5]. Morrison *et al.* have proposed that there is a correlation between the white line ratio and the magnetic moment of iron atoms in alloys such that higher white line ratios correspond to larger magnetic moments [6,7]. Their result for  $Fe_{0.3}Y_{0.7}$  amorphous alloy [7] can be directly compared with our data, since, as they pointed out, iron atoms in the amorphous alloy are not randomly distributed, but form clusters involving 260 atoms, a size which is similar to our nanometer-sized  $\gamma$ -iron crystallites. They found that iron clusters with a small magnetic moment of  $0.42\mu_B$  per iron atom gave an  $L_3/L_2$  ratio of 2.3, which was lower than in  $\alpha$ -iron. If the  $\gamma$ -iron crystallites in the Fe/MgO composite are in a similarly low-spin state, one can expect the white line ratio of  $\gamma$ -iron crystallites to be similar to the  $Fe_{0.3}Y_{0.7}$  alloy. However, the presently observed  $\gamma$ -iron crystallites  $L_3/L_2$  ratio is slightly larger than in  $\alpha$ -iron. Therefore, we conclude that the  $\gamma$ -iron crystallites embedded in our MgO films are in a high-spin state.

Two different electronic configurations for  $\gamma$ -iron have been proposed by Weiss [13]. One phase is a high-spin configuration (ferromagnetic coupling) with a large magnetic moment of  $2.8\mu_B$ . The other phase is a low-spin configuration (antiferromagnetic coupling) with a small magnetic moment of  $0.5\mu_B$ .

When  $\gamma$ -iron is in the high-spin state, it is ferromagnetic as mentioned above. Magnetic measurement on the present composite films showed ferromagnetic behavior [10], which can be considered as further evidence for a high-spin state of the  $\gamma$ -iron crystallites. Although it is known that a change of the magnetic phase of  $\gamma$ -iron is accompanied by a change of the lattice constant [13], according to recent theoretical work on magnetic properties of  $\gamma$ -iron [14], the behavior of the magnetic phase transition is rather complicated for lattice constants of around 0.36 nm. Therefore, it was not possible to determine the spin state of the  $\gamma$ -iron crystallites solely from the observed lattice constant of the crystallites.

As a final consideration, we comment on the possibility that there was an iron oxide layer surrounding the  $\gamma$ -iron crystallites in the composite films, which caused an increase in the white line ratio. Careful inspection of interface (surface) regions of  $\gamma$ -iron crystallites in MgO by using high resolution images such as figure 1a shows no evidence of additional layers. Further, no diffraction spots from iron oxide layers such as  $Fe_2O_3$ , or  $Fe_3O_4$ , were found in electron diffraction patterns, as shown in figure 1b. Unfortunately, absence of FeO is not easily established using diffraction patterns, as the structures of FeO and MgO are the same, and their lattice constants are similar ( $a_{FeO} = 0.428$  nm,  $a_{MgO} = 0.421$  nm). However, because FeO is usually antiferromagnetic, even if the  $\gamma$ -iron crystallites were covered with one or two FeO layers, the oxide could not contribute to the ferromagnetic behavior of composite films. The ferromagnetic properties of composite films thus must originate from the  $\gamma$ -iron crystallites, which are therefore in a high-spin state. The reasons for the appearance of the high spin state are most likely (1) a small lattice expansion [15,16], especially at the interface with the MgO matrix, and (2) the small size ( $d = 1 \sim 2$  nm) of the  $\gamma$ -iron crystallites.

We summarize our observations and compare them to previous work correlating the magnetic moment to the  $L_3/L_2$  ratio of various iron compounds in figure 5. The  $\gamma$ -iron magnetic moment entered in the figure is the one proposed by Weiss [13]. We also note that the present study confirms that EELS can be useful for studying the spin state of materials, and indicates that small  $\gamma$ -iron crystallites embedded in single-crystal MgO are in a high-spin state.

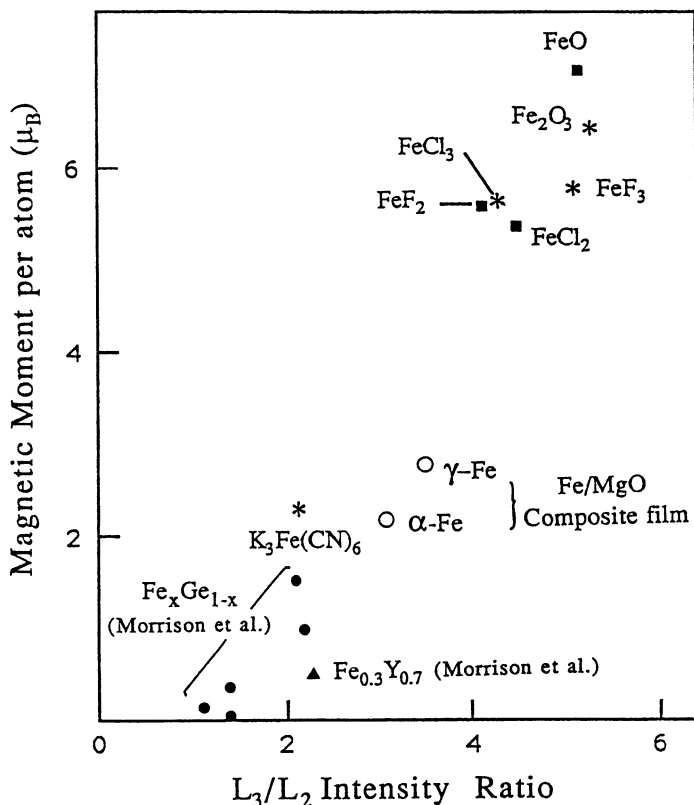


Fig. 5. — Correlation between the magnetic moment  $\mu_B$  per atom and the white line ratio for various iron materials. The data for the amorphous alloys and the iron compounds are taken from references [6,7] and [17], respectively. Materials with a large  $\mu_B$  show a large white line ratio.

### Acknowledgements.

The authors wish to express their thanks to prof. T. Kobayashi of Kyoto University and Prof. K. Mihama of Nagoya University for their encouragement throughout this work, are grateful to Mr. F. Yoshizaki for sample preparation, and thank Dr. O.L. Krivanek for revising their English.

### References

- [1] LEAPMAN R.D. and GRUNES L.A., *Phys. Rev. Lett.* **45** (1980) 397.
- [2] HORSLEY J.A., *J. Chem. Phys.* **76** (1989) 1451.
- [3] SPARROW T.G., WILLIAMS B.G., RAO C.N.R. and THOMAS J.M., *Chem. Phys. Lett.* **108** (1984) 547.
- [4] WADDINGTON W.G., REZ P., GRANT I.P. and HUMPHREYS C.J., *Phys. Rev.* **B34** (1986) 1467.
- [5] THOLE B.T. and VAN DER LAAN G., *Phys. Rev.* **B38** (1988) 3158.
- [6] MORRISON T.I., BODSKY M.B., ZALUZEC N.J. and SILL L.R., *Phys. Rev.* **B32** (1985) 3107.
- [7] MORRISON T.I., FOILES C.L., PEASE D.M. and ZALUZEC N.J., *Phys. Rev.* **B36** (1987) 3739.
- [8] PEARSON D.H., FULTZ B. and AHN C.C., *Appl. Phys. Lett.* **53** (1988) 1405.
- [9] MANOUBI T., TENCÉ M. and COLLIEX C., *Ultramicroscopy* **28** (1989) 49.

- [10] YOSHIKAZI F., TANAKA N. and MIHAMA K., *J. Electron Microsc.* (1990) in print.
- [11] PEARSON W.B., "Handbook of Lattice Spacings" (London, Pergamon Press, 1958).
- [12] EGERTON R.F., "Electron Energy Loss Spectroscopy in the Electron Microscope" (Plenum Press, 1986).
- [13] WEISS R.J., *Proc. Phys. Soc.* **82** (1963) 281.
- [14] WANG C.S., KLEIN B.M. and KRAKAUER H., *Phys. Rev. Lett.* **54** (1985) 1852.
- [15] KEUNE W., EZAWA T., MACEDO W.A.A., GLOS V., SCHLETZ K.P. and KIRSCHBAUM U., *Physica* **B161** (1989) 269.
- [16] MACEDO W.A.A. and KEUNE W., *Phys. Rev. Lett.* **61** (1988) 4 75.
- [17] KURATA H., NAGAI K., ISODA S. and KOBAYASHI T., Proc. 12th Int. Cong. on Electron Microscopy **2** (1990) 28.